COMPARATIVE STUDY OF GREEN SYNTHESIZED SILVER NANOPARTICLES USING DIFFERENT PLANT EXTRACTS OF INDIAN HABITAT WITH THEIR ANTI-MICROBIAL EFFICIENCIES

S. PARMAR[#], A.K. SINGH

https://www.doi.org/10.59277/RJB.2025.1.02

"Veer Kunwar Singh" University Ara, Bihar, India, [#]e-mail: saurabh1993parmar@gmail.com

Abstract: Green synthesis of silver nanoparticles using cloves (*Sygzium aromaticum*), cinnamon bark (*Cinnamomum cassia*) and tulsi (*Ocimum teniflorum*) leaves have been comparatively studied by different characterization tools, both in aqueous and powdered form. The uniformity in the concentration and physiochemical conditions has been maintained in all the three cases. The clove-based synthesized silver nanoparticles show the best outcomes in terms of stability, morphology, etc., whereas the cinnamon-based synthesized nanoparticles show the least standard of expected outcomes. It is here also noted that the synthesis has been carried out at normal pH, room temperature, and using very easily available instruments and apparatus. There has been intended to synthesize qualitative silver nanoparticles at ground level, using Indian plant extracts. Thus, the merit of this work is the process has been confined to very simple and basic requirements. The anti microbial applications have been analyzed and their efficiencies have been explained at both gram-negative and gram-positive types of bacteria.

Key words: Green synthesis, cloves, cinnamon, tulsi, characterization, gram-negative, gram-positive.

INTRODUCTION

In present era, nanoscience is a revolutionary field of material science. Today, nanomaterials are being used in every sphere, having tremendous impact in our lives. The nano sized particles exhibit unique properties as compared to their atomic or bulk level. The noble metals like silver, gold, platinum exhibit these specific properties at nanoscale such as localized surface plasmon resonance (LSPR) [9], enhanced permeability retention (EPR) effect, enhanced surface to volume ratio, etc. more boldly and nobly. Thus, the noble metal nanoparticles synthesis is

Received: October 2024;
in final form February 2025

comparatively easier and worthy. The paper presents here the green synthesis of silver nanoparticles, using precursor as $AgNO_3$ salt and reducing agents as three different plant extracts of Indian habitat i.e. cloves, cinnamon bark and tulsi leaves. The suitability and yielding has been taken into account by studying them using different characterization tools.

Silver is a noble metal with anti-microbial properties. There has been use of silver metal in form of bhashmas, in our ancestral background [15]. These silver nanoparticles in the form of bhashmas were being used as boosters for nervous and brain weakness, ointments for skin diseases, deranging drug for vata and pitta, etc. In today's world, these silver Nanoparticles still have the potential in many fields of daily use applications. Clove [3]is an Indian continent herb. It is a plant of *Myrtaceae* family, having species name *Sygzium aromaticum*. It contains various phytochemicals, among which eugenol is the main component present in it. Holy basil (tulsi) [1] is another common herb found in every indian household. It is a plant of *Lamiaceae* family, having species name *Ocimum tenuiflorum*. It contains querectin as the main reducing agent. Cinnamon bark [5] is a daily use spice of indian kitchen. Its species name is *Cinnamomum cassia* and it contains cinnamaldehyde as the main reducing agent.

Green synthesis [6] method has been adopted to synthesize silver nanoparticles. It is a bottom-up approach in which plants having phytochemicals reduce and stabilize the silver nanoparticles. Recently, many studies have proved that the plant extracts act as a potential precursor for the synthesis of nanomaterial in non-hazardous ways. Since the plant extract contains various secondary metabolites, it acts as reducing and stabilizing agents for the bio reduction reaction to synthesize novel metallic nanoparticles. Thus, it is an eco-friendly, one pot-one step process, which can efficiently produce quality nanoparticles.

The characterizations have been done using variety of characterization tools, which are UV-Vis analysis, zeta potential, dynamic light scattering (DLS) analysis, Fourier transform infrared (FTIR) analysis, X-ray diffraction (XRD) analysis, field emission scanning electron microscopy (FESEM) and energy dispersive spectroscopy (EDX) analysis. These tools confirm the formation of silver nanoparticles. The antimicrobial activities are studied using disc diffusion method [18], in agar medium at room temperature, using freshly cultured bacteria *E. coli* [13] (gram-negative bacteria) and *S. aureus* [8] (gram-positive bacteria). The synthesized silver nanoparticles show the bacterial growth inhibition in all the three cases, with different efficiencies.

MATERIALS AND METHODS

Silver nitrate ($AgNO_3$) 99% pure, molecular weight 169.87 gram (Research lab company cat. no. 01333) as shown Figure 1, has been bought from local chemical shop. About 20 gram each clove buds *(Sygzium aromaticum)* shown in Figure 2 and cinnamon bark (*Cinnamomum cassia*) shown Figure 3 have been brought from local grocery shop. About 20 gram tulsi also known as holy basil (*Ocimum teniflorum*) leaves shown in Figure 4 have been collected from the university garden premise. Double distilled water (DDW) has been used as aqueous medium and ethanol (95% pure) has been used as cleaning and washing agent. Whatman's No. 1 filter paper (Cytiva company Cat No. 1001-125) has been used for filter purpose.

Simple laboratorial equipment like hot plate magnetic stirrer, centrifugal machine (max 15000 rpm), where rpm is rotation per minute, digital pH meter, digital thermometer, digital milligram weighing machine, etc. have been used. All the experiment has been carried out at the temperature range 30 ºC – 50 ºC, in dust free and direct sunlight restricted environment.

3 mM concentrated aqueous solution of silver nitrate ($AgNO_3$) is prepared by mixing 750 mg of the $AgNO_3$ salt in 1500 mL of double distilled water. The solution is gently rotated at 1000 rpm on hot plate magnetic stirrer for 10 minutes. The solution is stored at room temperature.

Fig. 1. Silver nitrate salt.

Fig. 2. Clove buds.

Fig. 3. Cinnamon.

Fig. 4. Tulsi leaves.

The three different plant extracts of cloves, cinnamon and tulsi are prepared separately. Each 20 g of the plant stuffs (cloves, cinnamon bark, tulsi) are washed twice with double distilled water (DDW) and once with ethanol to remove any dust particles. Then the each of the three plant stuffs is heat dried at a temperature of 40 ºC, for 10 min, to evaporate the moisture. After that the plant stuffs are smashed and powdered separately using mortar and pestle, sieved and mixed them separately in three beakers each containing 250 mL of DDW. The three solutions are separately

heated at a temp of 50 ºC for 15 min. The solutions are twice filtered using Whatman's no. 1 filter paper and about each 150 mL of the plant extracts are stored in refrigerator at a temperature of 10 ºC.

The 1500 mL of 3 mM aqueous silver nitrate solution is divided equally into three parts, each of 500 mL. Each of the silver nitrate solution is mixed with 50 mL of the plant extract solutions i.e. in ratio 10:1. The three mixtures are gently stirred at a temperature of 40 ºC for 5 min. The mixtures in the case of tulsi and clove-based synthesis is start turning into suspension with cloudy formation. In the case of cinnamon, the mixture is getting somewhat darker in color only after heating it at 50 ºC for 5 minutes. The mixtures are incubated for 24 hours at room temperature, to get mixtures fully reduced.

After 24 hours color change can be witnessed in all the three mixtures as shown in Figure 5. The color change is the first evidence that the reduction has been occurred, because color changing is the phenomenon related to LSPR (localized surface plasmon resonance), which comes into action at nano level only.

(a) (b) (c)

Fig. 5. Photograph of color change due to LSPR after 24 h: (a) $AgNO_3$ + clove, (b) $AgNO_3$ + cinnamon, (c) $AgNO_3$ + tulsi.

OBTAINING POWDERED SAMPLE

Samples are centrifuged at 10,000 rpm for 10 min. The sediment clayey particles are collected and washed twice with ethanol. Afterward, the particles are heat dried at a constant temperature of 50 ºC for about 15 min. The powdered form obtained from each of the 500 mL of the prepared samples is about 80 mg in the case of cinnamon and about 100 mg in the case of tulsi and cloves. It is here observed that the nanoparticles are still in suspension form in large quantity, which further needs to be left for considerable amount of time to settle down and centrifuge again.

RESULTS

UV-VIS SPECROSCOPY ANALYSIS

Ultraviolet visible spectroscopy is a basic tool to characterize the nanoparticles by studying the absorbance of electromagnetic radiation in the range 300 to 800 nm. The analysis has been done 24 hours after the synthesis. The absorbance range is set in 0 to 1 range. As shown in the Figure 6, the graphs have been plotted absorption wavelength versus absorbance intensity. The peak values have been shown in table 1. In all the three cases, there is a peak in the range 450 nm to 500 nm, confirming the formation of nanoparticles [16] in aqueous solution. The absorbance intensity is nearly 0.5, which is indicating that the solutions are neither too concentrated nor too diluted.

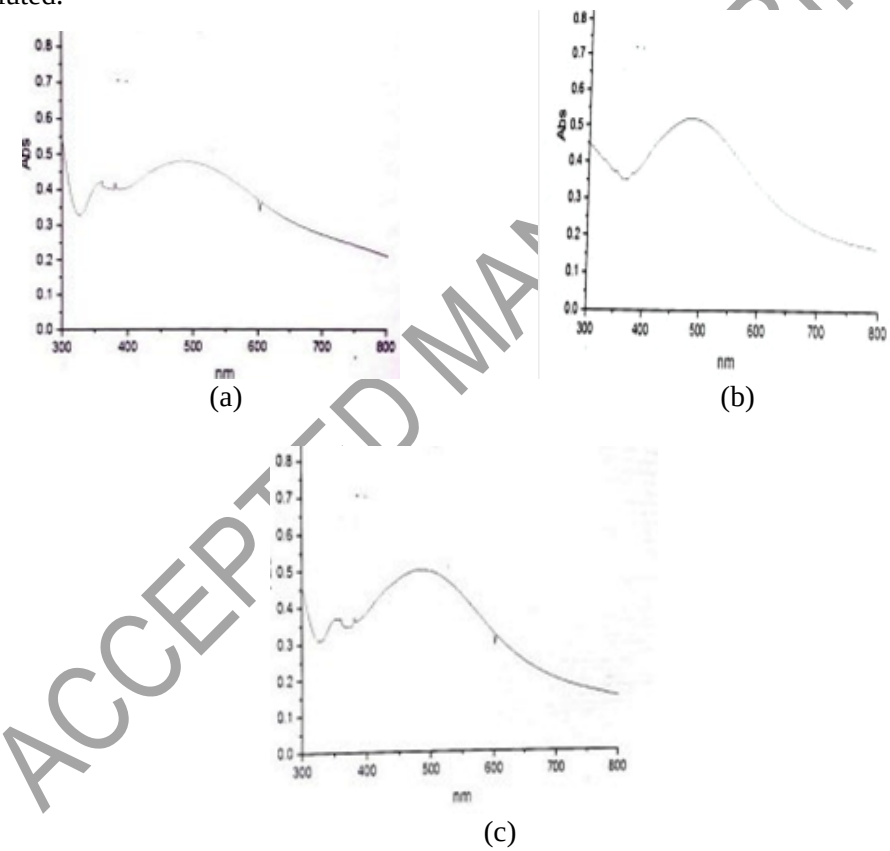

Fig. 6. UV-Vis graph analysis of (a) $AgNO_3$ + clove (b) $AgNO_3$ + tulsi (c) $AgNO_3$ + cinnamon.

Table 1

Ultraviolet-visible spectroscopy peaks (after 24 Hours)

Sample	Absorbance value (%)	Peak value (nm)
$AgNO_3$ + clove	55	500

$AgNO_3$ + tulsi	50	492
$AgNO_3$ + cinnamon	50	480

FOURIER TRANSFORM INFRARED ANALYSIS

Fourier transform infrared analysis is a characterization tool which can detect the functional group present in the solutions, responsible for reducing the silver nanoparticles. The analytical graphs as shown in Figure 7, have been plotted for wave number versus transmittance percentage. The peaks have been matched with standard reference Coates interpretation [2]. And the interpretation data has been shown in Table 2. It is clear that synthesized nanoparticles are enveloped by various phytochemicals having functional groups of alcohols, alkynes, ketones, amides, present in the different plant extracts. The broad peaks are the evidence that there are hydrogen bonds in the solution.

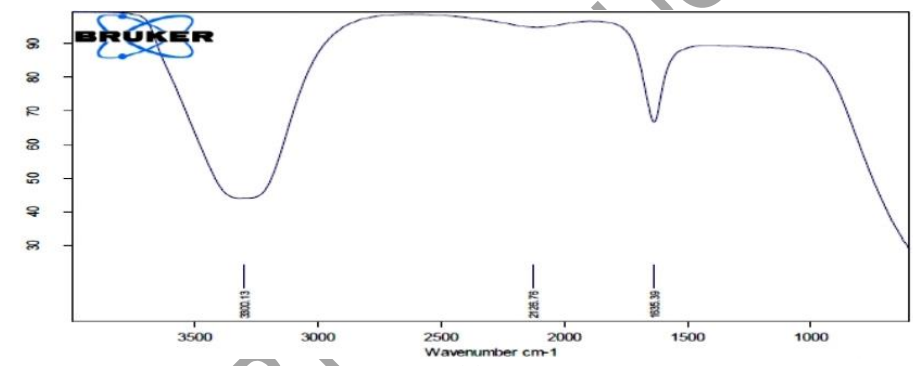

(a)

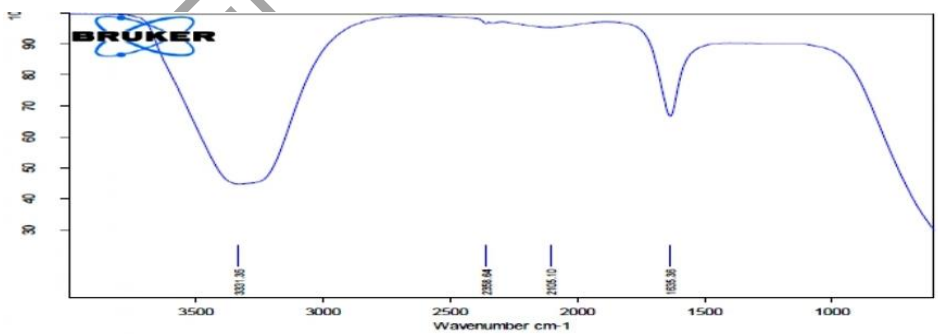

(b)

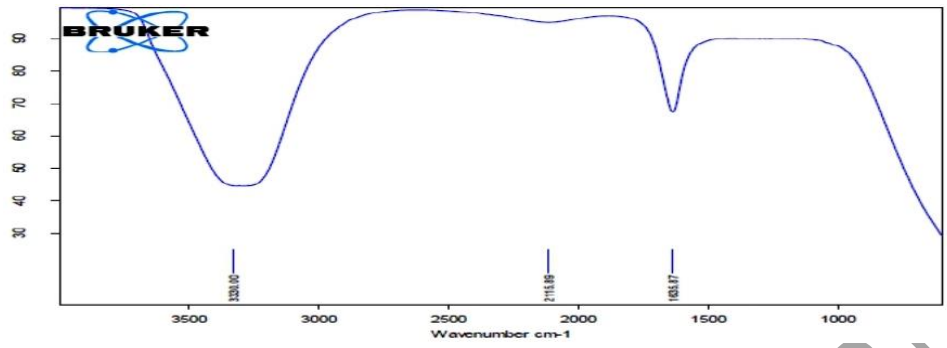

(c)

Fig. 7. FTIR absorption graph of: (a) $AgNO_3$ + clove, (b) $AgNO_3$ + tulsi, (c) $AgNO_3$ + cinnamon.

Table 2

FTIR peak interpretation

Peak wavenumber (cm^{-1})	Absorption (%)	Intensity of peak	Shape of the peak	Functional group from standard reference
3330.00	60	Strong	Broad	Normal polymeric OH stretch (Hydroxy group)
2115.89	8	Weak	Broad	C ≡ C terminal alkyne
1635.87	30	Medium	Sharp	$CONH_2$ amide

ZETA POTENTIAL ANALYSIS

The aqueous samples have been done zeta potential analysis, after 30 days of the synthesis, to test the stability of the samples in aqueous form. Zeta potential analyzer measures the potential difference between the surface of a solid particle immersed in a conducting liquid and the bulk of the liquid. The Figure 8 show the zeta potential [11] for all the three samples. The analysis has been presented in the Table 3. It can be concluded that even after 30 days, the tulsi-based nanoparticles are the most stable with the negative zeta potential of −18.08 mV and the cinnamon-based nanoparticles are the least stable with zeta potential of −7.65 mV.

Table 3

Zeta potential analysis and interpretation

Sample	Zeta potential	Interpretation
AgNp + tulsi solution	–18.08 mV	Moderate stability
AgNp + clove solution	–14.23 mV	Incipient stability
AgNp + cinnamon solution	–7.65 mV	Incipient instability

AgNp = silver nanoparticles.

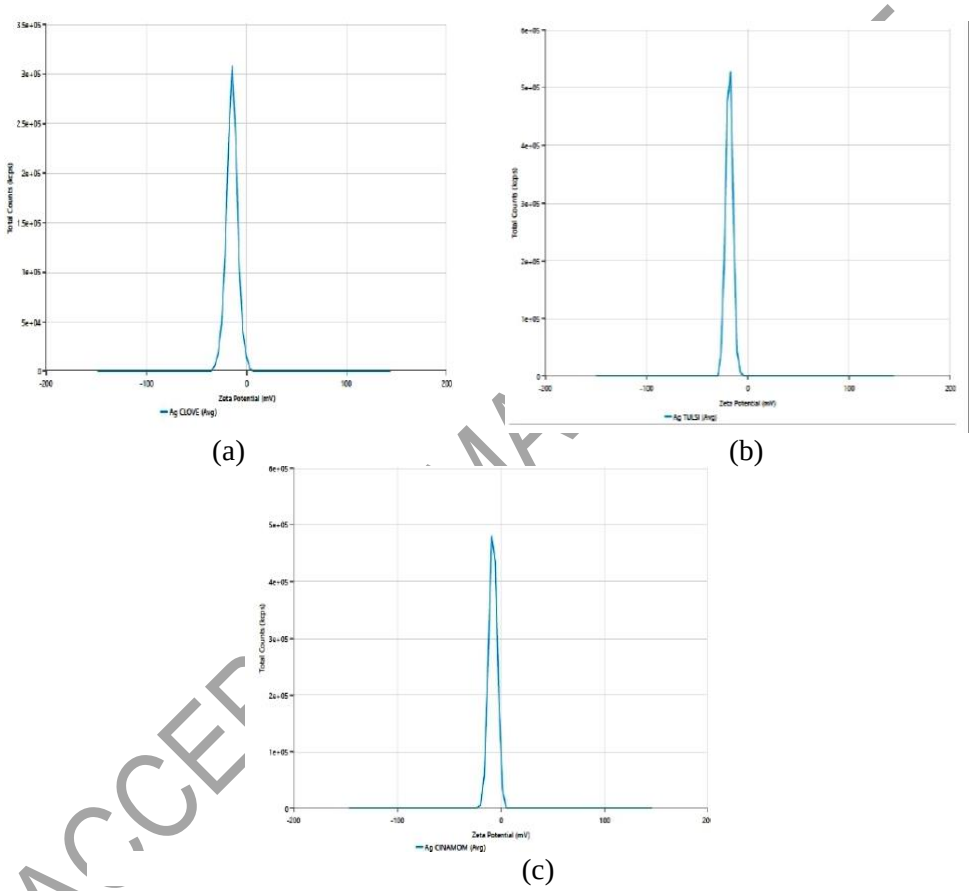

(a) (b)

(c)

Fig. 8. Zeta potential of (a) $AgNO_3$ + clove, (b) $AgNO_3$ + tulsi, (c) $AgNO_3$ + cinnamon.

DYNAMIC LIGHT SCATTERING ANALYSIS

Dynamic light scattering [13] (DLS) is an important tool which estimates the particle size in aqueous medium. It tells us about the particle size by detecting the intensity of scattered light and how much light has passed. Figure 9 shows the graph

of zeta size (nm) versus intensity (%) analysis. Table 3 sums up the result with the very big mean particle size of 434.5 nm, 192 nm and 287 nm for the tulsi, clove and cinnamon-based silver nanoparticles respectively. It may be attributed to the aggregation of nanoparticles exists after several days of the synthesis in nanoparticle suspension, and that is why the measured value of particle size are big in measurement [4].

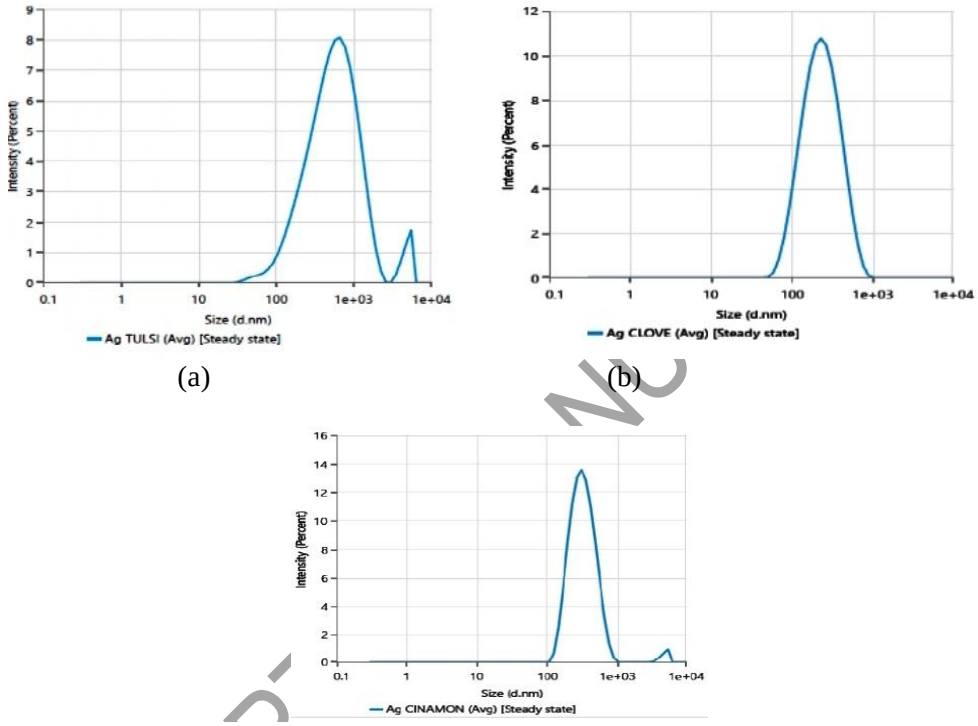

Fig. 9. DLS analysis of (a) $AgNO_3$ + tulsi, (b) $AgNO_3$ + clove, (c) $AgNO_3$+ cinnamon.

In the statistics Table 4 polydispersity index (PDI) gives the idea of the particles of varied sizes in the dispersed phase of a disperse system. The acceptable PDI for nanoparticles is between 0.2 to 0.3 range.

Table 4

DLS zeta size interpretation

Sample	Mean zeta size (nm)	Polydispersity index
Silver Np + tulsi	434.5	0.44
Silver Np + clove	192.0	0.23
Silver Np + cinnamon	287.4	0.25

That means the tulsi-based silver nanoparticles are too polydispersed, which may be due to the high concentration of reducing agent or precursor taken. But the clove and tulsi-based silver nanoparticles can be said to be largely mono dispersed in the aqueous medium.

Further characterizations have been done in powdered form of the samples.

X-RAY DIFFRACTION ANALYSIS

X-ray diffraction (XRD) characterization is the most widely used technique to determine the lattice parameters of the crystal. Size of the nanoparticles is calculated using Scherer equation [7]. Figure 10, 11 and 12 shows the XRD crystallography of three samples respectively. The powdered sample shows modest crystallite size indicated by the large number of diffraction peaks. Figures show the peaks at nearly 38 º, 44 º, 64 º, 77 º which are linked with the diffraction lattice planes of (111), (200), (220) and (311) respectively, which is in the good agreement with the crystal lattice XRD card (JCPDS file No. 04-0783) [16].

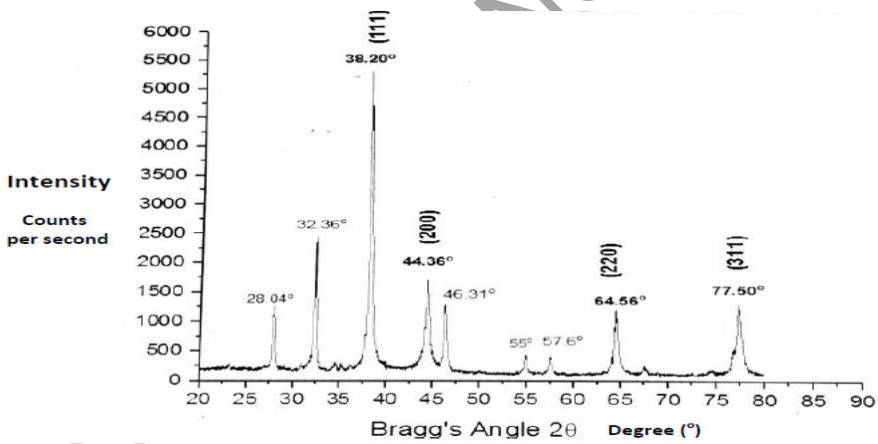

Fig. 10. XRD crystallography of silver nanoparticles of sample $AgNO_3$ + tulsi.

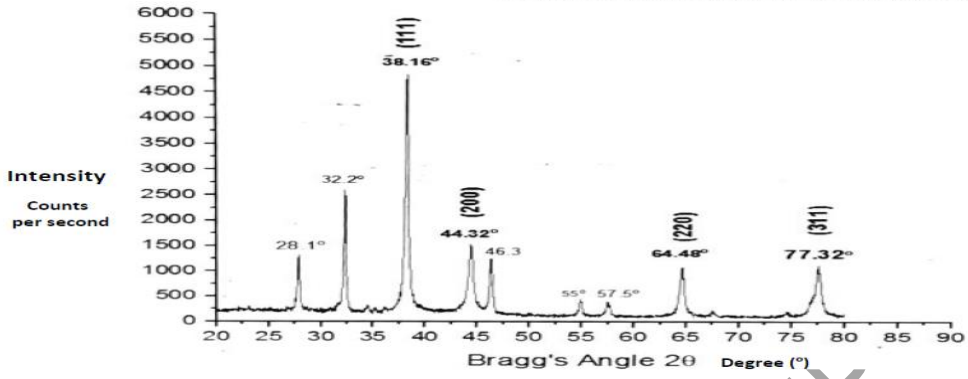

Fig. 11. XRD crystallography of silver nanoparticles of sample $AgNO_3$ + clove.

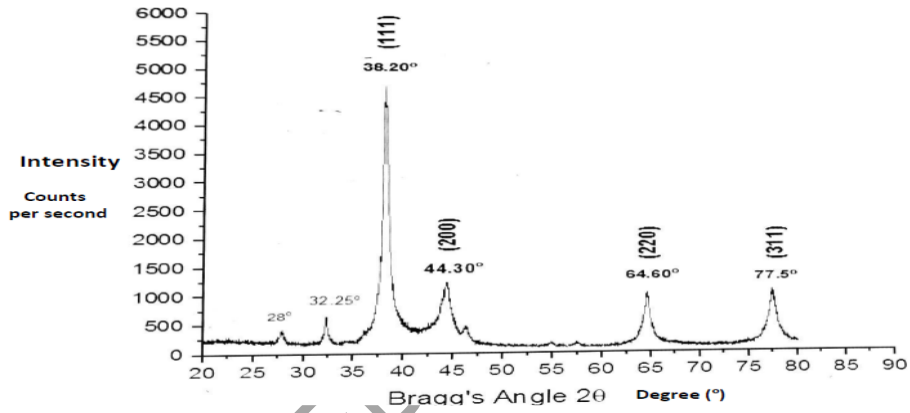

Fig. 12. XRD crystallography of silver nanoparticles of sample $AgNO_3$ + cinnamon.

In addition to these four peaks of face centered cubic (FCC) silver particles, there are some additional peaks (28 º, 32 º, 46 º, 55 º, 57 º) observed which may be due to the unreduced $AgNO_3$. Thus, all the three samples show crystallite structures in powdered form.

Scherer's Equation gives the crystalline diameter (size), as shown in Table 5.

$$D = \frac{k\lambda}{\beta \cos\theta} \quad (1)$$

where D = crystal diameter, k = 0.9, λ = 0.15 nm (X-ray), β = full width at half maximum (FWHM)(rad).

Table 5

Nanoparticle crystal diameter calculation

Peak angle 2Θ (°)	Intensity	Θ(°)	cosΘ	FWHM(°)	FWHM (β) (rad)	Crystal diameter (nm)

38.16°	4860	19.08°	0.94506	0.41	0.0071	20.11
44.32°	1546	22.16°	0.92613	0.58	0.0101	14.43
64.48°	1060	32.24°	0.84582	0.56	0.0097	16.45
77.32°	1081	38.66°	0.78021	0.64	0.0111	15.46

Bragg's law [10] gives interplanar spacing, as presented in Table 6.

$$d = \frac{n\lambda}{2\sin\theta} \quad (2)$$

where d = interplanar spacing, n = 1, λ = 0.15 nm (X-ray wavelength).

Lattice parameter gives the dimension of FCC cube :

$$a = d\,(h^2 + k^2 + l^2)^{1/2} \quad (3)$$

where a = lattice parameter, h, k, l = Miller indices.

Covalent radius for FCC structure :

$$r = \frac{a}{2\sqrt{2}} \quad (4)$$

where r = covalent radius**,** a = lattice parameter.

Table 6

Nanoparticle covalent radius calculation

Peak angle 2Θ (°)	Θ (°)	sin Θ	Miller indices *hkl*	$h^2+k^2+l^2$	Lattice parameter *a* (nm)	NP radius *r* (nm)
38.16	19.08	0.326	111	3	0.400	0.141
44.32	22.16	0.377	200	4	0.395	0.140
64.48	32.24	0.533	220	8	0.396	0.140
77.32	38.66	0.625	311	11	0.397	0.140

FESEM ANALYSIS

Field emission scanning electron microscope (FESEM) has been used to see the shape and morphology of nanoparticles in the powdered form. The samples have been tested at 4 magnifications of 10 K X, 25 K X, 50 K X and 100 K X as shown in Figure 13 for clove based synthesized silver nanoparticles. Figure 14 and Figure

15 show the FESEM imaging of tulsi-based and cinnamon-based synthesized nanoparticles respectively. It can be seen that clove-based silver nanoparticles are showing the best morphology, whereas agglomeration can be seen in the case of cinnamon-based silver nanoparticles.

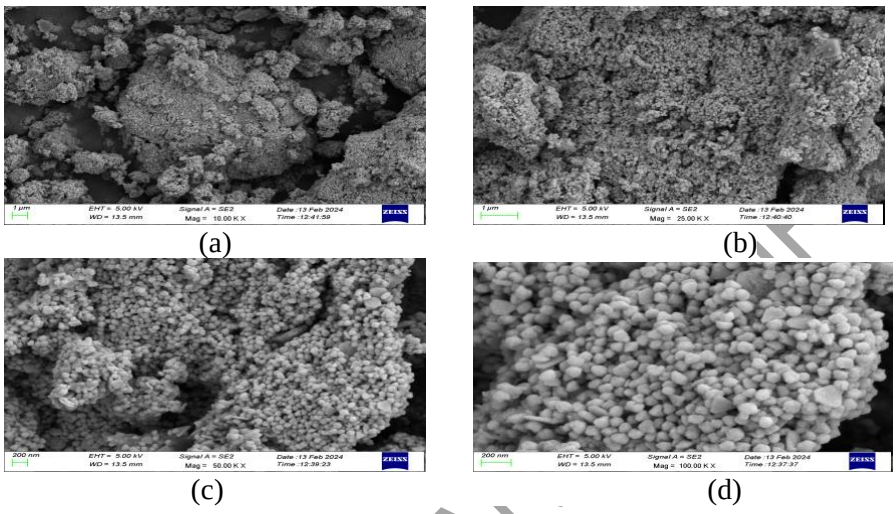

Fig. 13. FESEM imaging of cloves-based synthesized silver nanoparticles at (a) 10 KX, (b) 25 KX, (c) 50 KX, (d) 100 KX.

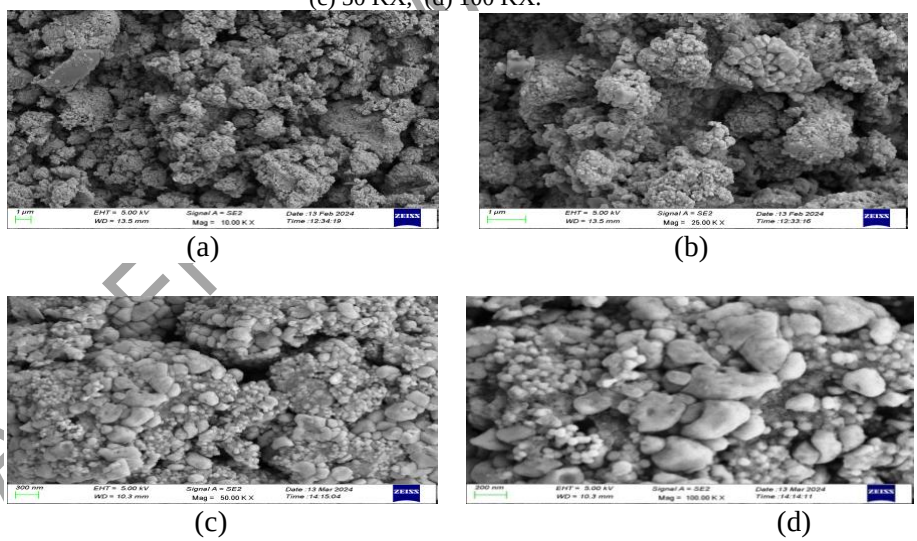

Fig. 14. FESEM imaging of tulsi-based synthesized silver nanoparticles at (a) 10 KX, (b) 25 KX, (c) 50 KX, (d) 100 KX.

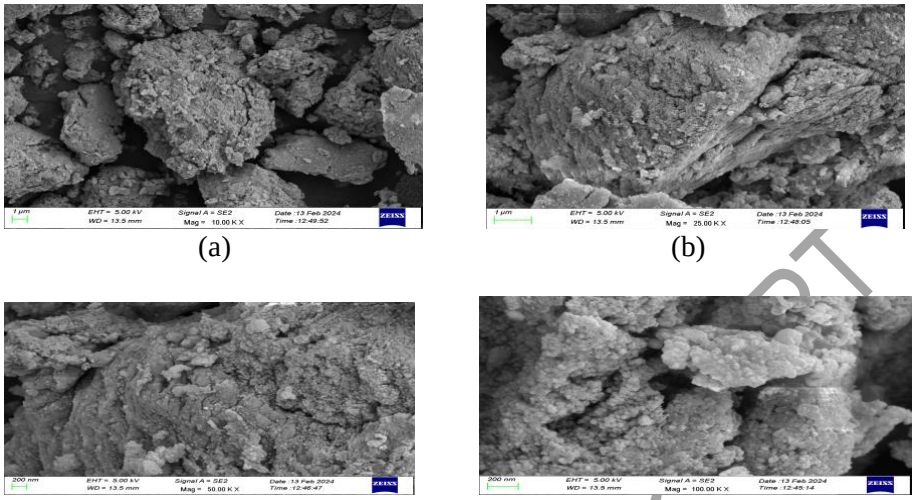

(a) (b)

(c) (d)

Fig. 15. FESEM imaging of cinnamon-based synthesized silver nanoparticles at (a) 10 KX, (b) 25 KX, (c) 50 KX, (d) 100 KX.

ENERGY DISPERSIVE X-RAY ANALYSIS

Energy dispersive X-ray (EDX) analysis is used to determine the elemental composition of the material. Through EDX, it will be confirmed that the above FESEM pictures are of silver nanoparticles. The units of the energy dispersive X-ray graph are keV on the x-axis *versus* the peak intensity on the y-axis. Figure 16 represents EDX report of tulsi-based synthesis of silver nanoparticles, with abundance of 81 % silver metal. Figure 17 represents EDX report of clove-based synthesis of silver nanoparticles, with abundance of 76 % silver metal. Figure 18 represents EDX report of cinnamon-based synthesis of silver nanoparticles, with abundance about 70 % silver metal.

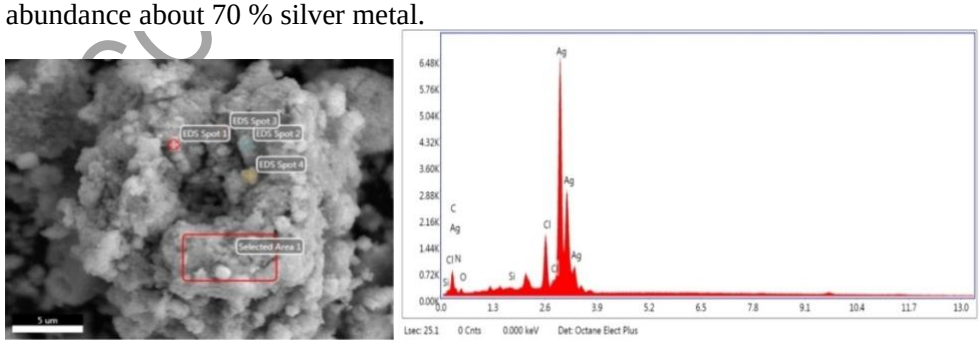

Fig. 16. EDX spot area and EDX report for tulsi-based synthesized silver nanoparticles.

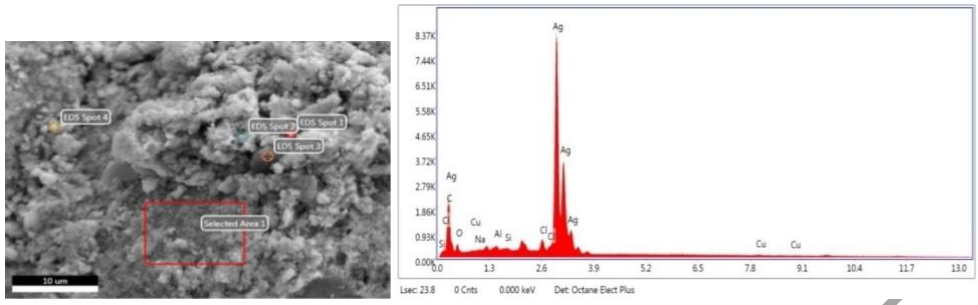

Fig. 17. EDX spot area and EDX report for clove-based synthesized silver nanoparticles.

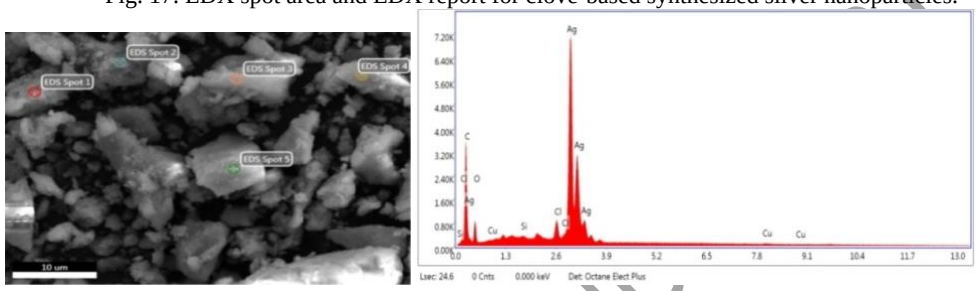

Fig. 18. EDX spot area and EDX report for cinnamon-based synthesized silver nanoparticles.

ANTIBACTERIAL ACTIVITY ANALYSIS

Anti microbial activities of the samples have been done by disc diffusion method on the agar medium. The freshly prepared aqueous cultured bacteria have been used and incubation have been done at 37 ºC, at ambient oxygen supply, for 24 hours.

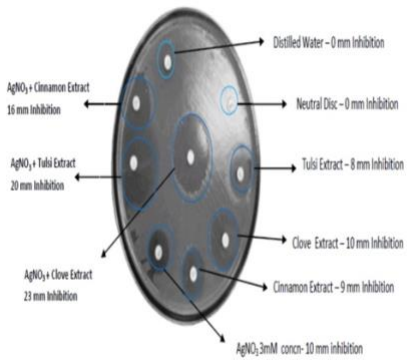

Fig. 19. *S. aureus* bacterial testing.

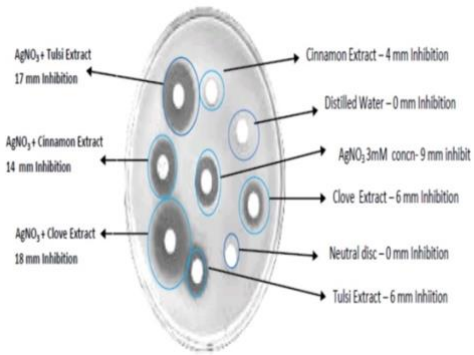

Fig. 20. *E. coli* bacterial testing.

Both stains of bacteria have been tested. That is one gram-positive bacteria *Staphylococcus aureus* (Fig. 19) and one gram-negative bacteria *Escherichia Coli* (Fig. 20) have been separately examined with 100 µL of the samples. Total 8 types of samples as shown in Table 7 have been tested. The inhibition diameter is measured using milli meter measuring scale. All the three samples are proved to be

microbe-resistant. But the cloves-based silver nanoparticles prove to be the most promising nanoparticles as they are the most effective both on gram negative and gram-positive bacteria.

The mechanism [17] of the anti bacterial effect of the silver nanoparticles may be attributed as the silver nanoparticles permeate the cell membrane of the bacteria and attack the ribosomes and disturb the functioning of bacteria metabolism. Smaller particles having larger surface area provides more bacteria killing impact.

Table 7

Anti-microbial analysis report

Samples taken for anti-microbial testing (100 µL)	Zone of inhibition for *S. aureus* (mm)	Zone of inhibition for *E. coli* (mm)
Distilled water	No inhibition	No inhibition
Tulsi extract	8	6
Clove extract	10	6
Cinnamon extract	9	4
$AgNO_3$ solution (3 mM conc.)	10	9
$AgNO_3$+clove extract	23	18
$AgNO_3$+tulsi extract	20	17
$AgNO_3$+cinnamon extract	16	14

CONCLUSION

From the above discussion, we find that using a very simple approach we can synthesize anti microbial silver nanoparticles, using cloves, cinnamon and tulsi leaves. These nanoparticles may be used to produce anti septic ointments anti pathogen medicines, after testing the suitability factor to the human body. Despite lapsing several days, these highly concentration-based synthesized nanoparticles are capped and stabilized up to a great extent. Comparatively, the clove-based nanoparticles show less stability in the aqueous medium, but in powdered form they show the best morphology. Cinnamon proves to be the least capable reducing agent and there are impurities more in this case. There are further possibilities to be tested at different Ph, temperature and other physio chemical conditions. For the present work, we can conclude that the silver nanoparticles can be synthesized taking the precursor and the reducing agent in the higher concentration and with a very basic

technique. These nanoparticles can be further researched for the nano layer deposits electronic material [14] such as sensors, etc.

Acknowledgements. The author (Saurabh Parmar) is obliged to Dr. Anil Kr. Singh (Professor, Deptt. of Physics, VKSU Ara) as a mentor, without whom the aim would be impossible to achieve and the whole PG department of Physics, VKS Ara as a collaborative institution, where the experiments have been carried out. The author extends his gratitude to the whole members of PG Department of Chemistry, VKS University Ara, for guidance and support on several occasions in chemistry approach. In addition, the author would like to thank SAIF Centre and ME department of IIT Patna (Bihta Campus, Bihar) where the characterizations have been done.

REFERENCES

1. BHATTACHARYA, D., T. K. SUR, JANA, Holy Basil (*Ocimum sanctum* Linn.) and Its Efficacy in Various Health Conditions: An Overview, *Pharmacognosy Journal*, 2021, **13**(2), 365–374, https://doi: 10.5530/pj.2021.13.47.
2. COATES, J., Interpretation of infrared spectra: A practical approach, In: R.A. Meyers, ed., *Encyclopedia of Analytical Chemistry, John Wiley & Sons Ltd.*, Chichester, 2000, pp. 10815–10837, https://doi:10.1002/9780470027318.a5606.
3. HOWDEN, B.P., S.G. GIULIERI, T.W.F. LUNG, *Staphylococcus aureus* host interactions and adaptation, *Nature Review Microbiology*, 2023, **21**, 380–395, https://doi.org/10.1038/s41579-023-00852-y.
4. JIA, Z., J. LI, L. GAO, D. YANG, A. KANAEV, Dynamic light scattering: A powerful tool for *in situ* nanoparticle sizing, *Colloids* Interfaces, 2023, **7**(15), 1–18, https://doi.org/10.3390/colloids7010015.
5. KAISER, K.G., V. DELATTRE, V.J. FROST, G.W. BUCK, J.V. PHU, T.G. FERNANDEZ, I.E. PAVEL, Nanosilver: An old antibacterial agent with great promise in the fight against antibiotic resistance, *Antibiotics* (Basel), 2023, **12**(8), 1208–1264, https://doi: 10.3390/antibiotics12081264.
6. KHATUN, M., Z. KHATUN, R. KARIM, R. HABIB, H. RAHMAN, A. AZIZ, Green synthesis of silver nanoparticles using extracts of *Mikania cordata* leaves and evaluation of their antioxidant, antimicrobial and cytotoxic properties, *Food Chemistry Advances*, 2023 **3**, 100386-394, https://doi.org/10.1016/j.focha.2023.100386.
7. MORELHAO, S. L., S. W. KYCIA, A simple formula for determining nanoparticle size distribution by combining small-angle X-ray scattering and diffraction results, *Acta Crystallographica Section A*, 2022, **78**(5), 459–462, https://doi.org/10.1107/S2053273322007215.
8. MOSTAFA, A., T. YASSIN, A.A. ASKAR, F.O. AL-OTIBI, Phytochemical analysis, activities antiproliferative and antifungal of different *Syzygium aromaticum* solvent extracts, *Journal of King Saud University – Science*, 2023, **35**(1), 102362-368, https://doi.org/10.1016/j.jksus.2022.102362.
9. NANDA, B.P., P, RANI, P. PAUL, AMAN, S. S. GANTI, R. BHATIA, Recent trends and impact of localized surface plasmon resonance (LSPR) and surface-enhanced Raman spectroscopy (SERS) in modern analysis, *Journal of Pharmaceutical Analysis*, 2024, *In press*, https://doi.org/10.1016/j.jpha.2024.02.013.

10. OMORI, N.E., D.A. BOBITAN, A. VAMVAKEROS, M.A. BEALE, D.M.J. SIMON, Recent developments in X-ray diffraction/scattering computed tomography for materials science, *Philosophical Transactions of the Royal Society A*, 2023, **381**, A.38120220350, http://doi.org/10.1098/rsta.2022.0350.
11. PORTELA, R., A. SERRANO-LOTINA, P. BAEZA, V. ALCOLEA-RODRIGUEZ, M. VILLAROEL, P. AVILA, Zeta potential as a tool for functional materials development, *Catalysis Today*, 2023, **423**, 113862-873, https://doi.org/10.1016/j.cattod.2022.08.004.
12. RODRIGUEZ-LOYA, J., M. LERMA, J.L. GARDEA-TORRESDEY, Dynamic light scattering and its application to control nanoparticle aggregation in colloidal systems: A review, *Micromachines* (Basel), 2023, **15**(24), https://doi: 10.3390/mi15010024.
13. RUIZ, N., T.J. SILHAVY, How *Escherichia coli* became the flagship bacterium of molecular biology, *Journal of Clinical Microbiology*, 2022, **204**, e00230-22, https://doi.org/10.1128/jb.00230-22.
14. SHEHAWY, A.S. EL., A. ELSAYED, O.A. EL-SHEHABY, E.M. ALI, Potentiality of the green synthesized silver nanoparticles for heavy metal removal using *Laurencia papillosa* seaweed, *Egyptian Journal of Aquatic Research*, 2023, **49**(4), 513–519, https://doi.org/10.1016/j.ejar.2023.10.001.
15. THAKUR, S.K., R. PAL, P. PANDEY, R. YADAV, I. GUPTA, R.K. MALAKAR, H.S. CHAWRA, The anti oxidant cinnamon, other phyto-containing compounds including their application in various diseases, *Asian Journal of Phytomedicine and Clinical Research*, 2022, **10**(4), 124–140.
16. UMADEVI, M., S. SHALINI, M.R. BINDHU, Synthesis of silver nanoparticle using *D. carota* extract, *Advances in Natural Sciences*: *Nanoscience and Nanotechnology*, IOP Publishing, 2012, **3**, 1–6, https://doi: 10.1088/2043-6262/3/2/02500.
17. WASILEWSKA, A., U. KLEKOTKA, M. ZAMBRYZYCKA, G. ZAMBROWSKI, I. SWIECICKA, B. KALSKA-SZOSTKO, Physico-chemical properties and antimicrobial activity of silver nanoparticles fabricated by green synthesis, *Food Chemistry*, 2023, **400**, 133960-966, https://doi.org/10.1016/j.foodchem.2022.133960.
18. WEBER, D.M., M.A. WALLACE, C.D. BURNHAM, Stop waiting for tomorrow: Disk diffusion performed on early growth is an accurate method for antimicrobial susceptibility testing with reduced turnaround time, *Journal of Clinical Microbiology*, 2022, **60**, e03007-20, https://doi.org/10.1128/jcm.03007-20.